

## Human *in Vivo* Pharmacokinetics of [<sup>14</sup>C]Dibenzo[*def,p*]chrysene by Accelerator Mass Spectrometry Following Oral Microdosing

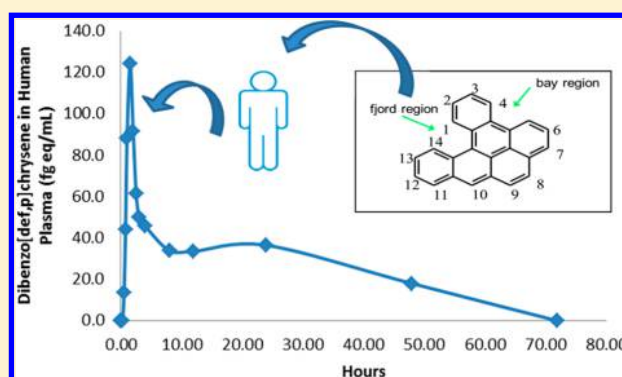
Erin Madeen,<sup>†,‡</sup> Richard A. Corley,<sup>‡,⊥</sup> Susan Crowell,<sup>‡,⊥</sup> Kenneth Turteltaub,<sup>#</sup> Ted Ognibene,<sup>¶</sup> Mike Malfatti,<sup>#</sup> Tammie J. McQuistan,<sup>§</sup> Mary Garrard,<sup>‡,§,||</sup> Dan Sudakin,<sup>†,‡,||</sup> and David E. Williams<sup>\*,†,‡,§,||</sup>

<sup>†</sup>Department of Environmental and Molecular Toxicology, <sup>‡</sup>Superfund Research Center, <sup>§</sup>Linus Pauling Institute, and <sup>||</sup>Environmental Health Sciences Center, Oregon State University, Corvallis, Oregon 97331, United States

<sup>⊥</sup>Systems Toxicology & Exposure Science, Pacific Northwest National Laboratory, Richland, Washington 99354, United States

<sup>#</sup>Biology and Biotechnology Research Division, and <sup>¶</sup>the Center for Accelerator Mass Spectrometry, Lawrence Livermore National Laboratory, Livermore, California 94550, United States

**ABSTRACT:** Dibenzo[*def,p*]chrysene (DBC), (also known as dibenzo[*a,l*]pyrene), is a high molecular weight polycyclic aromatic hydrocarbon (PAH) found in the environment, including food, produced by the incomplete combustion of hydrocarbons. DBC, classified by IARC as a 2A probable human carcinogen, has a relative potency factor (RPF) in animal cancer models 30-fold higher than benzo[*a*]pyrene. No data are available describing the disposition of high molecular weight (>4 rings) PAHs in humans to compare to animal studies. Pharmacokinetics of DBC was determined in 3 female and 6 male human volunteers following oral microdosing (29 ng, 5 nCi) of [<sup>14</sup>C]-DBC. This study was made possible with highly sensitive accelerator mass spectrometry (AMS), capable of detecting [<sup>14</sup>C]-DBC equivalents in plasma and urine following a dose considered of *de minimus* risk to human health. Plasma and urine were collected over 72 h. The plasma  $C_{max}$  was  $68.8 \pm 44.3$  fg·mL<sup>-1</sup> with a  $T_{max}$  of  $2.25 \pm 1.04$  h. Elimination occurred in two distinct phases: a rapid ( $\alpha$ )-phase, with a  $T_{1/2}$  of  $5.8 \pm 3.4$  h and an apparent elimination rate constant ( $K_{el}$ ) of  $0.17 \pm 0.12$  fg·h<sup>-1</sup>, followed by a slower ( $\beta$ )-phase, with a  $T_{1/2}$  of  $41.3 \pm 29.8$  h and an apparent  $K_{el}$  of  $0.03 \pm 0.02$  fg·h<sup>-1</sup>. In spite of the high degree of hydrophobicity (log  $K_{ow}$  of 7.4), DBC was eliminated rapidly in humans, as are most PAHs in animals, compared to other hydrophobic persistent organic pollutants such as, DDT, PCBs and TCDD. Preliminary examination utilizing a new UHPLC-AMS interface, suggests the presence of polar metabolites in plasma as early as 45 min following dosing. This is the first *in vivo* data set describing pharmacokinetics in humans of a high molecular weight PAH and should be a valuable addition to risk assessment paradigms.



### INTRODUCTION

Polycyclic aromatic hydrocarbons (PAHs) are produced by the incomplete combustion of carbon and are of concern as environmental toxicants/carcinogens.<sup>1</sup> The most recent list of the priority chemicals at remediation sites by the Agency for Toxic Substances Disease Registry (ATSDR) includes individual PAHs or PAH mixtures as three of the top 10 chemicals of concern.<sup>2</sup> Major sources of environmental exposure include wood smoke, creosote, and burning of fossil fuels and tobacco.<sup>1</sup> PAHs consisting of four rings or less constitute the low molecular weight, volatile class. These PAHs tend to be less toxic and are typically classified as level 3 or insufficient weight of evidence as carcinogens in humans.<sup>1</sup> The major route of exposure to low molecular weight PAHs, such as naphthalene, pyrene, and phenanthrene, is inhalation. The high molecular weight PAHs include five or more aromatic rings. The majority of exposure (>95%), to high molecular weight PAHs in nonsmokers, is through the diet in a variety of foods including breads and cereal grains, vegetables, and smoke-cured or barbecued meats.<sup>3–5</sup> The high molecular weight group contains

the majority of the carcinogenic PAHs, including benzo[*a*]pyrene (BaP, class 1, known human carcinogen) and dibenzo[*def,p*]chrysene (DBC, CAS 191-30-0, class 2A, probable human carcinogen).<sup>1</sup>

Dietary intake of total PAHs in the U.S. has been estimated to be between 160 and 1600 ng/day.<sup>6</sup> Some studies have reported intake levels of BaP alone at 40–2800 ng/day.<sup>7,8</sup> A 2005 report from the FAO/WHO Joint Expert Committee on Food Additives and Contaminants listed a mean BaP daily dietary intake of 280 ng per 70 kg individual with 700 ng considered as a high-level intake.<sup>9</sup> Finally, a report by Menzie et al. estimated total carcinogenic PAH intake at 3120 ng/day for a nonsmoking male, 19–50 years of age, of which 96.2% was from the diet.<sup>10</sup> The European Union established a maximum limit for BaP in smoked meats at 5,000 ng/kg fresh weight.<sup>3</sup> Data on DBC contamination of food is scarce. Veyrand et al. addressed DBC (also known as dibenzo[*a,l*]pyrene) as a

Received: September 29, 2014

Published: November 24, 2014

component of food from a French market, estimating a daily exposure of 0.129 ng/kg BW in French adults and 0.208 ng/kg BW in French children.<sup>11</sup>

Crowell et al. developed a physiologically based pharmacokinetic (PBPK) model for DBC and BaP, relying upon previous studies of *in vitro* (human and rodent liver) BaP metabolism and the metabolic profile *in vivo* following oral gavage in rodents.<sup>12</sup> Administering an oral dose of 15 mg/kg DBC to mice resulted in a  $T_{\max}$  between 2 and 4 h, with detectable DBC in blood 48 h post gavage. The  $T_{1/2}$  was found to be between 3.4 and 4.8 h.<sup>12,13</sup> The higher log  $K_{ow}$  of DBC (7.4), compared to that of BaP (6.1), is believed to contribute to a prolonged sequestration in blood and other tissues. The DBC model development relied heavily upon BaP due, in part, to the lack of available data on DBC metabolism.

Accelerator mass spectrometry (AMS) measures the ratio of  $^{14}\text{C}/\text{C}$  with  $^{14}\text{C}$  detection limits in the attomole range per mg total carbon,<sup>14,15</sup> allowing the use of a “microdose”, defined as a dose at least 2 orders of magnitude below that which would be expected to yield a pharmacological effect. AMS is increasingly being utilized by pharmaceutical companies to assess pharmacokinetic parameters, metabolism, and excretion in humans during drug development (Phase 0 trials).<sup>16–18</sup> These studies almost exclusively utilized  $^{14}\text{C}$  as the radiolabel, and doses of 100  $\mu\text{Ci}$  have been standard.<sup>17</sup> AMS is an attractive method to determine human pharmacokinetics, DNA binding, and other potential biomarkers of importance in risk assessment of compounds with potential toxicity. For example, AMS has been utilized to determine DNA binding of [ $^{14}\text{C}$ ]-labeled amino acid pyrolysis products or cooked meat mutagens, MeIQ, PhIP, MeIQx,<sup>19–22</sup> as well as BaP<sup>23</sup> and the pharmacokinetics of the potent human dietary hepatocarcinogen, aflatoxin B<sub>1</sub>.<sup>24</sup> The sensitivity provided by AMS allows for safe microdosing of human volunteers with chemical carcinogens, such as DBC, at environmentally relevant doses, providing pharmacokinetic parameters for risk assessment that do not rely solely on high-dose animal studies.

In this study, we determined the human *in vivo* pharmacokinetics of DBC, following microdosing, utilizing AMS. Total elimination of DBC<sub>eq</sub> (parent and metabolites), detected as [ $^{14}\text{C}$ ], are used to determine the pharmacokinetics in plasma and urine. Solid sample AMS is not able to distinguish between labeled parent compound and metabolites. Total plasma distribution and urinary elimination are compared to total plasma distribution and urinary elimination scaled from rodent models.

## EXPERIMENTAL PROCEDURES

**Human Volunteers.** All protocols and procedures, including plans for recruitment and volunteer informed consent documents, were approved by the OSU Institutional Review Board. The use of radioisotopes was reviewed and approved by an OSU Radioactive Use Agreement under the oversight of the Oregon Health Authority. Healthy adult males and infertile (postmenopausal or tubally ligated) females, between the ages of 20–65, were recruited for this study. To protect confidentiality, all specimens were deidentified at the time of collection.

Additional inclusion criteria were as follows: good general health; nonsmoking; not using medications that can affect gut motility; and no history of gastrointestinal surgeries, kidney or liver disease, gastrointestinal diseases such as Crohn’s, ulcerative colitis, or gastritis. A medical examination was conducted by a licensed physician. The screening assessment included a careful menopausal history and a urine pregnancy test for all women. Women who were pregnant or

capable of becoming pregnant were excluded from the study in an abundance of caution, due to the proven transplacental toxicity of DBC in high dose rodent models.<sup>25–31</sup> A total of 9 volunteers were enrolled. Individual body weight, height, BMI, age, gender, ethnicity, and race were recorded (Table 1).

**Table 1. Volunteer Demographics**

	BW (kg)	Ht (cm)	BMI	age	gender	ethnicity	race
V1	85	173	28	45	F	non-Hispanic	Asian
V3	99	188	28	45	M	non-Hispanic	Caucasian
V5	86	158	34	65	F	non-Hispanic	Caucasian
V6	94	196	24	47	M	non-Hispanic	Caucasian
V8	78	180	24	26	M	non-Hispanic	Caucasian
V9	78	156	32	56	F	non-Hispanic	Caucasian
V10	71	174	23	20	M	non-Hispanic	Caucasian
V11	113	180	35	43	M	non-Hispanic	Caucasian
V13	124	191	34	36	M	non-Hispanic	Caucasian

**Justification of the Dose Used in This Study.** The 29 ng DBC dose utilized in this study is equivalent to the BaP content of a 5.2 oz. serving of smoked meat at the European Union maximum legal limit<sup>3</sup> or 28% of the average daily dietary PAH intake.<sup>10</sup> This chemical dose was chosen to be relevant to typical dietary exposure in humans. The specific activity of [l-ring-U- $^{14}\text{C}$ ]-DBC was 51.4 nCi/nmol, resulting in 5 nCi of [ $^{14}\text{C}$ ] in a 29 ng dose. This  $\beta$  particle radiation dose of 5 nCi can be compared to the internal radiation of consuming 5 bananas, each containing 1 nCi [ $^{40}\text{K}$ ].<sup>32</sup> It would require a dose of 200 study capsules to equal the radioactive dose of a single [ $^{14}\text{C}$ ]-urea diagnostic test for *Helicobacter pylori*.<sup>33</sup> The radioactive dose was chosen to be detectable by AMS without appreciable risk to volunteers consistent with the policy of utilizing doses as low as Reasonably Achievable (ALARA) or Practical (ALARP).<sup>34</sup>

**Chemicals.** Dibenz[*defp*]chrysene (formerly known as dibenz[*a,l*]pyrene) [l-ring-U- $^{14}\text{C}$ ], MRI Part No. U479C, 51.4 mCi/mmol, was obtained from the NCI Chemical Carcinogen Standards Reference Repository, Midwest Research Institute (Kansas City, MO). The reagents used include Ultima Flo M scintillation cocktail, sulfuric acid, HPLC grade acetonitrile, Milli-Q water, ethyl acetate, potassium sulfate, 95% ethanol (PCCA 50–3161), lactose monohydrate (PCCA 30-3329) and size 0 cellulose capsules (Spectrum, Irvine CA). Chromatography utilized a Luna 3  $\mu\text{m}$  particle C<sub>18</sub> 100 Å 150 × 3 mm Phenomenex HPLC column with a C<sub>18</sub> 2 mm guard column on an Agilent 1100 HPLC with UV detector.

**[ $^{14}\text{C}$ ]-DBC Dosing Solution.** A portion of the stock solution of [ $^{14}\text{C}$ ]-DBC (1.11 mCi/ml, 6.53 mg/mL benzene) was blown to dryness under argon and then purified, prior to the preparation of dosing solutions, to  $\geq 99\%$  radiochemical purity via reverse phase-HPLC. HPLC elution conditions were isocratic 90% ACN, 10% H<sub>2</sub>O with a flow rate of 1 mL/min at a column temperature of 35 °C. The A<sub>280</sub> peak containing purified [ $^{14}\text{C}$ ]-DBC (6.0 to 6.5 min retention time) was collected over several HPLC runs. The pooled eluent was evaporated to dryness under a stream of argon and resuspended in ethanol thrice to produce the dosing solution. An HPLC run of the dosing solution was collected in 15-s fractions for scintillation counting to assess radioactive purity ( $\geq 99\%$ ). The dosing solution was diluted with additional ethanol to 0.16 nCi/ $\mu\text{L}$ , representing a final target dose of 29 ng DBC/30  $\mu\text{L}$  dose incorporated into each cellulose capsule. The stock solution was stored at  $-80$  °C under argon and protected from light. All neat DBC powder was handled by a trained carcinogen

Table 2. Total Nanograms of [<sup>14</sup>C]-DBC<sub>eq</sub> Eliminated in Urine during Each Collection Interval<sup>a</sup>

	0–6 h	6–12 h	12–24 h	24–48 h	48–72 h	elim. total	oral dose DBC (ng)	% excreted
V1	0.085	0.049	0.044	0.046	0.006	0.230	23.9	0.96
V3	0.044	0.109	0.038	0.029	0.000	0.220	24.5	0.90
V5	0.033	0.184	0.123	0.119	0.073	0.532	25.2	2.11
V6	0.179	0.075	0.107	0.056	0.024	0.441	29.8	1.48
V8	0.071	0.046	0.111	0.058	0.000	0.285	23.9	1.20
V9	0.052	0.028	0.063	0.043	0.014	0.200	28.5	0.70
V10	0.237	0.104	0.097	0.027	0.028	0.494	25.6	1.93
V11	0.113	0.059	0.052	0.056	0.017	0.297	29.7	1.00
V13	0.124	0.056	0.045	0.033	0.005	0.263	28.5	0.92
average								1.24
SD								0.49

<sup>a</sup>[<sup>14</sup>C]-DBC<sub>eq</sub> elimination (ng) per total urine volume in a given pooled time point. The percent excreted is reported as the total urine elimination divided by the total oral dose.

specialist in an enclosed glovebox, per the OSU Extreme Carcinogen handling protocol. DBC solutions were stored in a locked laboratory dedicated to carcinogens, and all waste was discarded in accordance with OSU radiation safety and hazardous material protocols.

**Capsule Manufacturing and Quality Control.** Capsules were prepared by filling empty cellulose capsules with pharmaceutical grade lactose monohydrate. Thirty microliters of 0.16 nCi/ $\mu$ L dosing solution was applied to the capsule and sealed by allowing the ethanol to evaporate, inverting the capsule to create a lactose layer above the dosing solution to prevent any possible integrity loss upon moistening, and the capsule cap was pinched closed over the capsule body. Every capsule batch manufactured included a dosing capsule per volunteer plus at least 3 extra for quality control. Capsules were stored at  $-20^{\circ}\text{C}$  until time of use and utilized within 5 days of preparation. Quality control was performed by scintillation counting 3 randomly chosen capsules per batch, individually dissolved by vortex in 5 mL of water prior to the addition of 15 mL of scintillation cocktail. The variability between capsules per batch was  $\leq 5\%$ . The exact dosage a volunteer received, measured by scintillation, is included in Table 2.

**Dosing and Sample Collection Protocols.** At 8 a.m., volunteers who had fasted overnight were orally administered a cellulose capsule containing <sup>14</sup>C-DBC (target dose of 29 ng DBC, 5 nCi <sup>14</sup>C), which was swallowed with 100 mL of water. Food and water were made available at 10 a.m. Blood was drawn by a registered nurse at 0, 0.25, 0.5, 0.75, 1.0, 1.5, 2.0, 2.5, 3, 4, 8, 12, 24, 48, and 72 h post-consumption and collected into glass vacutainer tubes containing the anticoagulant, EDTA. An indwelling i.v. catheter was used for the first 4 h of blood collection; the remaining time points were collected by needle sticks. Initial studies using whole blood for AMS analysis resulted in high signal-to-noise based upon background endogenous C that obscured the <sup>14</sup>C attributable to [<sup>14</sup>C]-DBC. Therefore, whole blood was centrifuged for 10 min at 1,000g and 0.75 mL plasma aliquots transferred to glass culture tubes containing 0.75 g of K<sub>2</sub>SO<sub>4</sub> to prevent emulsion, and stored at  $4^{\circ}\text{C}$  until extracted for AMS analysis. Urine contains low endogenous carbon, allowing AMS analysis directly without extraction. Additional plasma and urine specimens were stored at  $-80^{\circ}\text{C}$  for archiving.

All urine voided during the 72-h cycle was collected. Urine was pooled by 0–6, 6–12, 12–24, 24–48, and 48–72 h batches for homogenized sampling and volume record by pool. Glass urine containers were provided for *as voided* collection. Coded plasma and plasma extracts and urine samples were stored at  $-20^{\circ}\text{C}$  prior to shipment to Lawrence Livermore National Laboratory (LLNL) for analysis by AMS. Archived samples were stored at  $-80^{\circ}\text{C}$  at OSU.

**Extraction of Plasma and Collection of Urine.** Plasma samples were extracted according to the method of Crowell et al.<sup>12</sup> The samples were acidified with 0.75 mL of 0.9 M H<sub>2</sub>SO<sub>4</sub>, vortexed for 20 s, then extracted thrice with 1 mL of ethyl acetate, and centrifuged at 750g for 10 min. The combined extracts were evaporated under argon to dryness in an 8 mL amber glass vial with a PTFE cap liner, then stored at  $-20^{\circ}\text{C}$  until shipped on dry ice to LLNL for AMS analysis.

As PAHs can adsorb to plastic, care was taken to use glass containers (amber when possible) for protection from light and argon or nitrogen capping to prevent oxidation of samples. Urine was aliquoted in 1 mL volumes for shipping, requiring no additional processing prior to AMS preparation.

**Extraction Efficiency.** The extraction efficiency for [<sup>14</sup>C]-DBC from plasma was determined by spiking plasma with known amounts of [<sup>14</sup>C]-DBC using dilutions of the [<sup>14</sup>C]-DBC microdosing ethanol stock solution. Following ethyl acetate extraction and reconstitution with 50:50 methanol/water (v/v) used for AMS analysis (described below), the recovery was  $51 \pm 10\%$  ( $n = 3$ ) as determined by AMS. In a separate test of extraction efficiency, fresh or thawed frozen plasma, 0.75 mL, was spiked with 1.25 nCi [<sup>14</sup>C]-DBC solution prior to extraction resulting in  $55 \pm 7\%$  recovery of [<sup>14</sup>C]-DBC as detected by scintillation counting. This process was repeated with several [<sup>14</sup>C]-DBC concentrations and with detection by AMS and scintillation counting. Overall, across a number of concentrations,  $55 \pm 7\%$  (at the low end of previously reported recoveries of 61–101% in human studies with pharmaceuticals,<sup>18</sup> perhaps due to the much lower mass of the dose utilized in this study) was the average DBC recovery when reconstituted in methanol/water, and this value was used for efficiency corrections in the PK parameters reported below. Recent work by Crowell et al.<sup>35</sup> had determined this to be the optimal extraction method for DBC, as well as the diol, and tetraol metabolites.

**AMS of Plasma and Urine Samples.** Upon arrival at LLNL, samples were stored at  $-80^{\circ}\text{C}$  until processing. Plasma extract samples were reconstituted with 100  $\mu$ L of 50:50 methanol/water and converted to graphite by the method of Ognibene et al.<sup>36</sup> Urine samples (100  $\mu$ L) were converted, without prior processing, by the same graphitization method. The urine data was not normalized for creatinine. All voided urine was collected, pooled by time point, and volumetrically recorded prior to aliquoting and storing pooled samples. Briefly, the samples were evaporated and flame-sealed in a quartz tube containing Cu(II) and combusted to  $900^{\circ}\text{C}$ , producing CO<sub>2</sub>. The CO<sub>2</sub> is then transferred to a septa sealed glass tube containing Zn and Co and heated to  $525^{\circ}\text{C}$ , producing graphite on the Co catalyst. The graphite is then loaded into an aluminum sample holder for AMS analysis.

AMS analysis was conducted on the 1 MV AMS, constructed and maintained by the Center for Accelerator Mass Spectrometry at LLNL. The current AMS operating conditions are optimized to determine the ratio of <sup>14</sup>C/C with a precision of 3% and sensitivity of 0.4 attomol <sup>14</sup>C per mg of total carbon.<sup>37</sup> Solid sample standards containing <sup>14</sup>C/C content of  $1.5 \times$  modern are measured intermittently throughout the analysis to assess the ionization and counting efficiency of the spectrometer. The biochemical samples are measured 4–10 times with the collection of at least 10,000 <sup>14</sup>C counts or for 30 s each time.<sup>38</sup>

**Determination of Pharmacokinetic Parameters.** Pharmacokinetic analysis of data utilized an Excel based add-on developed at Allergan, Inc. (Irvine, CA).<sup>39</sup> Briefly, the formulas rely on non-compartmental analysis of six functions: peak concentrations in plasma

( $C_{\max}$ ), time of peak plasma concentration ( $T_{\max}$ ), plasma elimination half-life ( $T_{1/2}$ ), apparent elimination rate constant ( $k_{el}$ ), and area under the plasma concentration curve ( $AUC_{0-t}$  and  $AUC_{0-\infty}$ ) using standard regression techniques.<sup>40</sup> Alpha and beta phase classifications were based on peak to trough values. Urinary clearance (CL, mL/min) was calculated by dividing the cumulative amount of  $^{14}\text{C}$  eliminated in the urine over 72 h by the plasma  $AUC_{0-72h}$ .

## RESULTS

We were able to empirically determine the environmentally relevant *in vivo* pharmacokinetics of [ $^{14}\text{C}$ ]-DBC in human volunteers utilizing AMS. The pool of nine volunteers included both sexes and was characterized by an age range from 20 to 65 years of age and BMIs from 23 to 35 (Table 1). No recruitment selection was made by volunteer physical characteristics. This study was intended to assess the range of pharmacokinetics in a cross section of human volunteers; as such, it is not statistically powered to assess parameters such as gender, age, or BMI. Differences in age could lead to differences in gut motility, possibly resulting in changes in absorption. The range of BMI likely results in a range of blood volumes and distribution. Because of a necessary change in plasma collection and processing method, three volunteers were excluded from the plasma pharmacokinetic analysis (Table 3 and Figure 2); however, urine data from all nine volunteers are included (Table 2 and Figure 1).

There were some similarities in the temporal pattern (but not magnitude) of absorption/excretion between individuals (Figures 1 and 2). Levels of [ $^{14}\text{C}$ ] in plasma rose rapidly following oral administration of [ $^{14}\text{C}$ ]-DBC to volunteers that had been fasted overnight (Tables 3 and 4, and Figure 2).

A  $T_{\max}$  at 2.25 h was observed, followed by a rapid  $\alpha$ -phase elimination prior to a slower  $\beta$ -phase elimination. This study was limited to the appearance and disappearance of  $^{14}\text{C}$ -labeled DBC<sub>eq</sub> from plasma and the levels appearing with time in urine (a true mass balance study would have required fecal analysis as well as determination of tissue levels (not possible in a human study without subsequent diagnostic surgery)). Considering differences in absorption based on motility, distribution based on BMI, and metabolism based on polymorphisms, the pharmacokinetics were notably consistent.

Recovery of urinary  $^{14}\text{C}$  over 72 h yielded  $1.24 \pm 0.49\%$  of the dose administered (Table 2). Because of the high hydrophobicity ( $\log K_{ow}$  7.4), the majority of DBC is likely unabsorbed and eliminated in the feces unlike 3- or 4-ring PAHs, which were reported to be rapidly absorbed from the intestine.<sup>41</sup> However, if we had collected urine over a longer period and observed a pattern similar to plasma, it could be concluded that sequestered DBC is released slowly from the system. Oral bioavailability could be expected to be strongly linked to the fat content of vehicle administered at dosing.<sup>41,42</sup> The fasted volunteers administered a dosing capsule with water likely limited bioavailability. Previous high dosing studies of BaP in rodents have resulted in minimal elimination in urine, 0.22–0.35% and 0.10–0.08% of oral dose administered, detected as known metabolites.<sup>43,44</sup> Oral gavage of mice with 15 mg/kg of DBC with corn oil vehicle yielded 4.9 to 7% urinary excretion of the total oral dose.<sup>13</sup> Administering an oral dose of 15 mg/kg DBC to mice resulted in a  $T_{\max}$  between 2 and 4 h, with detectable DBC in blood 48 h post-gavage.

Table 3. Plasma Pharmacokinetics of DBC<sub>eq</sub> in Human Volunteers<sup>a</sup>

	$C_{\max}$ (fg·mL <sup>-1</sup> )	$T_{\max}^{\text{plasma}}$ (h)	$AUC_{0-t}$ (fg·h·mL <sup>-1</sup> )	$K_{el}$ (fg·h <sup>-1</sup> )	$AUC_{0-\infty}$ (fg·h·mL <sup>-1</sup> )	$T_{1/2}$ (h)	$\alpha$ -phase $T_{1/2}$ (h)	$\alpha$ -phase $K_{el}$ (fg·h <sup>-1</sup> )	$\alpha$ -phase $AUC_{0-t}$	$\beta$ -elim $T_{1/2}$ (h)	$\beta$ -elim $K_{el}$ (fg·h <sup>-1</sup> )	urinary DBC <sub>eq</sub> clearance CL (mL·min <sup>-1</sup> )
V1	124.1	1.50	1616	0.03	1616	23.5	6.8	0.10	462.1	23.6	0.03	59.4
V6	118.2	1.50	2850	0.03	3690	27.5	11.7	0.06	859.1	66.6	0.01	15.5
V8	30.4	1.50	589	0.03	699	23.9	4.8	0.14	179.7	28.3	0.02	48.5
V9	41.6	4.00	433	0.05	604	13.1	1.7	0.41	30.7	10.2	0.07	46.2
V10	75.0	2.00	1921	0.00	6578	142.2	5.8	0.12	236.9	88.6	0.01	25.7
V13	23.3	3.00	237	0.03	338	22.1	3.8	0.18	74.8	30.6	0.02	11.1
avg	68.8	2.25	1274	0.03	2254	42.1	5.8	0.17	307.2	41.3	0.03	51.0
SD	44.3	1.04	1027	0.02	2449	49.3	3.4	0.12	309.9	29.8	0.02	33.4

<sup>a</sup>Non compartmental analysis of pharmacokinetic parameters.

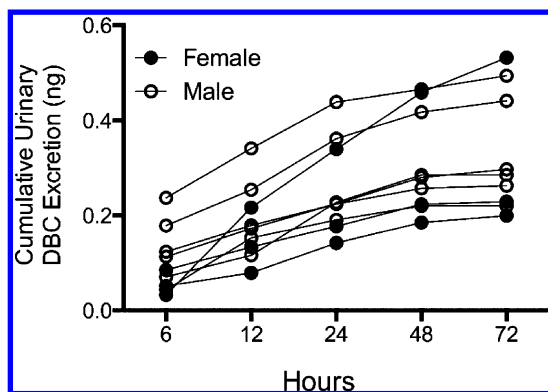


**Figure 1.** Cumulative urinary elimination of  $[^{14}\text{C}]\text{-DBC}_{\text{eq}}$  over time for six volunteers. All voided urine was collected over the 72 h of the study. A volumetric measurement was taken of urine pooled by time. A sample of 1 mL of urine was measured for  $[^{14}\text{C}]\text{-DBC}_{\text{eq}}$  by AMS per pool, as described in Experimental Procedures. Volumetric corrections were made for total  $[^{14}\text{C}]\text{-DBC}_{\text{eq}}$  elimination per pool. Results are recorded cumulatively.

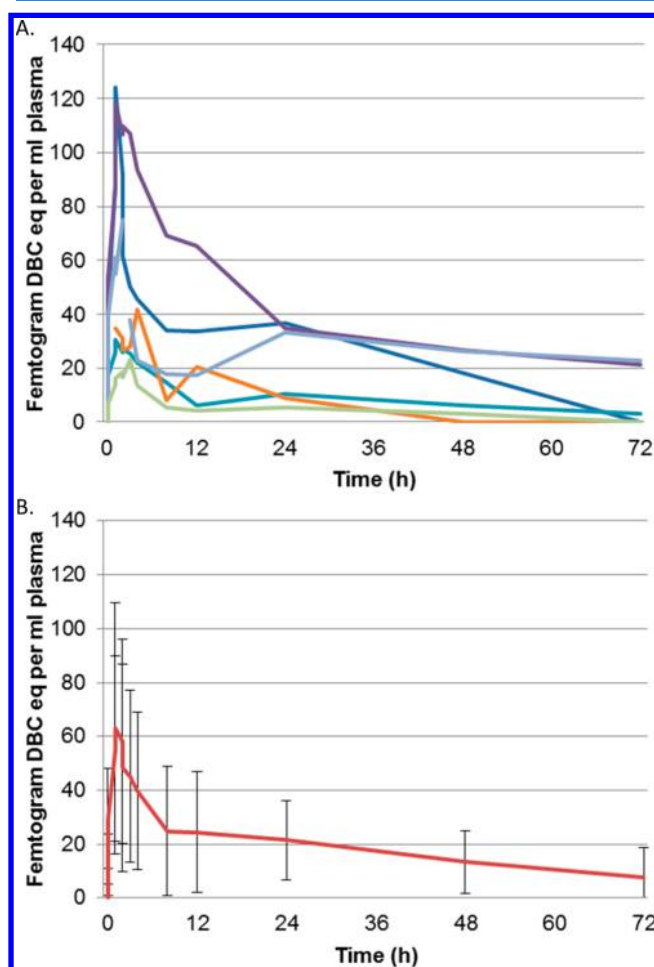


**Figure 2.**  $[^{14}\text{C}]\text{-DBC}_{\text{eq}}$  plasma elimination curve in 6 volunteers (A) and averaged (B). (A) Plasma levels of  $[^{14}\text{C}]\text{-DBC}_{\text{eq}}$  over time are depicted for 6 individual volunteers as measured by AMS as described in Experimental Procedures. (B) This graph depicts the average and standard deviation of  $[^{14}\text{C}]\text{-DBC}_{\text{eq}}$  in plasma for the same 6 volunteers as those in panel A.

## DISCUSSION

As environmental PAHs occur in complex mixtures, ingestion/elimination kinetics in humans from PAH exposures are difficult to discern. The translation of high dose animal experiment data for human risk assessment is often criticized as being of questionable relevance for human exposures. Because of the sensitivity of AMS, we are able to assess the *in vivo* human metabolic parameters of one of the most carcinogenic PAHs in animal models, DBC, while maintaining risk to volunteers at a *de minimus* level. Our pharmacokinetic data set following human DBC exposure at environmentally relevant levels offer an excellent biomonitoring tool for agencies charged with risk assessment and modeling to humans of high molecular weight carcinogenic PAHs.

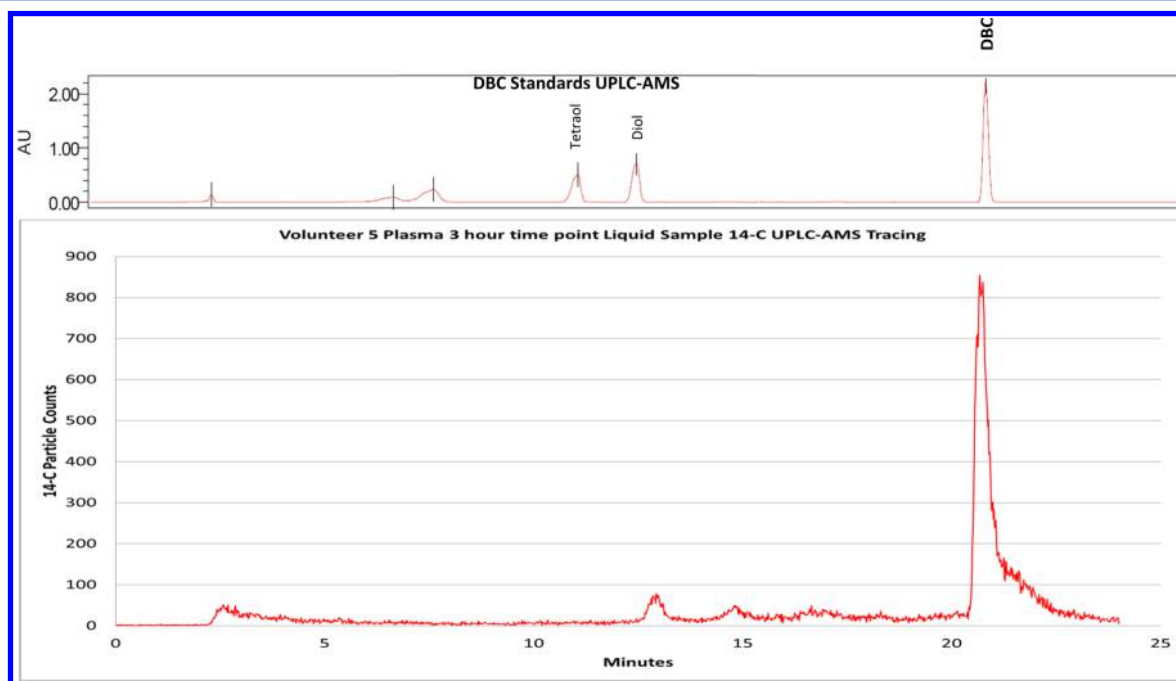
PAHs are pro-carcinogens, requiring enzymatic activation to electrophilic metabolites such as epoxides, dihydrodiol-epoxides, and quinones.<sup>45,46</sup> These electrophiles have numerous nucleophilic targets in the cell including DNA. In the case of DBC, cytochrome P450 (P450)-dependent 11,12-epoxygenation followed by hydrolysis (epoxide hydrolase) and a second epoxygenation produces the 11,12-dihydrodiol-13,14-epoxide (DBCDE). Of the four possible enantiomers, the (–)-*anti*-11R,12S-dihydrodiol-13S,14R-epoxide or (–)-*anti*-DBCDE is thought to be the most efficient at forming DNA adducts at a number of sites on purine bases<sup>47</sup> especially at N<sup>6</sup>-dA and N<sup>2</sup>-dG. Understanding the extent of metabolism, both bioactivation and detoxication (conjugation by SULTs, UGTs, and GSTs), following exposure to environmentally relevant doses would greatly add to the impact of Bio-AMS studies such as this one. The same is true for the determination of the extent and identity of DNA adducts in peripheral blood mononucleocytes following microdosing.

A current strength and drawback to the solid sample Bio-AMS technology employed in this study is that only total  $[^{14}\text{C}]$  label is detected. While providing sensitivity in the attomole range, this method is not capable of speciation, i.e., chemical identification and quantification of the parent compound and metabolites. Previously, to identify metabolites, plasma extracts would have to be separated by HPLC and collected as discrete fractions, based on the retention time of metabolite standards, prior to graphitization.<sup>14</sup> This approach is burdened with the same limitations of HPLC fraction collection for uncoupled traditional MS. HPLC fraction selection is based on the retention time of commercially available standards for downstream MS analysis. Only select fractions can be analyzed due to study limitations, including manual sample preparation.

New instrumentation at LLNL provides liquid sample AMS through the interface of UHPLC and AMS and determination of the metabolite profile.<sup>48</sup> Moving wire coupled UHPLC-Bio-AMS (liquid sample Bio-AMS) technology combusts column eluent to  $^{14}\text{CO}_2$ , prior to AMS carbon isotope detection across an entire chromatographic run. Parent, metabolite, and all conjugated species present from a biological matrix such as plasma, urine, or isolated DNA adducts can be detected and quantitated. Standards are necessary for identification based on retention time, but all species resulting from metabolism would be represented in the  $^{14}\text{C}$  tracing. Future work will focus on utilizing liquid sample Bio-AMS to identify the species and concentration of PAH metabolites over time and examination of interindividual differences such as genetics or previously environmental exposures, elucidating gene-environmental interactions at microdoses. One such study is currently underway

Table 4. Plasma DBC<sub>eq</sub> As Determined by AMS (fg DBC<sub>eq</sub>/mL Plasma)

time (h)	0.00	0.25	0.50	0.75	1.0	1.5	2.0	2.5	3.0	4.0	8.0	12.0	24.0	48.0	72.0
V1	0.0	0.0	13.8	44.1	88.4	124	91.7	61.5	50.1	45.7	33.8	33.6	36.5	18.0	0.0
V6	0.0	0.0	27.9	53.7	87.3	118	107	110	107	93.4	69.3	65.1	34.9	26.5	21.2
V8	0.0	0.4	6.7	17.4	25.9	30.4	25.7	26.9	25.6	22.1	14.8	6.1	10.3	6.2	3.2
V9	0.0	0.0	0.4	15.4	N.D. <sup>a</sup>	34.7	30.8	26.5	27.9	41.6	8.1	20.4	9.0	0.0	0.0
V10	0.0	8.9	23.7	39.5	61.1	54.8	75.0	N.D.	37.8	22.6	17.6	17.3	33.0	26.1	22.7
V13	0.0	0.0	1.4	7.1	13.9	16.1	18.6	16.5	23.3	13.4	5.2	4.3	5.5	3.2	0.0
mean	0.0	1.5	12.3	29.5	55.3	63.1	58.1	48.2	45.3	39.8	24.8	24.5	21.5	13.3	7.8
SD	0.0	3.6	11.6	18.7	34.4	46.7	37.8	38.4	31.9	29.0	24.0	22.6	14.7	11.7	11.0

<sup>a</sup>N.D., not detected.

**Figure 3.** UHPLC-AMS of [<sup>14</sup>C]-DBC and putative metabolites from plasma of volunteer 5 3 h following dosing. Plasma samples were extracted twice with 50  $\mu$ L of ethyl acetate and the extract transferred to an HPLC vial with a 300  $\mu$ L insert. The ethyl acetate was evaporated in a vacuum chamber and the residue reconstituted with 50  $\mu$ L of acetonitrile prior to injection. Five microliters of plasma extract (volunteer 5, 3 h after dosing) was injected onto a Phenomenex Kinetex 2.6  $\mu$ m C<sub>18</sub> 100  $\text{\AA}$  (Part no: 00f-4462-AN) column (150  $\times$  2.1 mm) fitted with a C<sub>18</sub> guard column and eluted with 45% acetonitrile for 0–3 min followed by a linear gradient (3–10 min) to 100% acetonitrile, which was maintained from 10 to 13 min before a return to initial conditions (flow rate of 0.12 mL·min<sup>-1</sup> (25 °C)). Following passage through a dual channel UV/vis detector (280 and 315 nm), the eluent was deposited onto a moving nickel wire and the [<sup>14</sup>C]-DBC<sub>eq</sub> converted to <sup>14</sup>CO<sub>2</sub> prior to AMS analysis.<sup>48</sup> Multiple channels allow for the simultaneous determination of A<sub>280</sub> and A<sub>315</sub> as well as counts of <sup>12</sup>C and <sup>14</sup>C. Only the <sup>14</sup>C profile is shown here. The use of unlabeled parent DBC and standards (DBC-( $\pm$ )-11,12-diol and DBC-( $\pm$ )-11,12,13,14-tetraol) allow for tentative identification of <sup>14</sup>C peaks (top panel). The polar putative metabolite eluting between 2 and 2.5 min is currently unknown but could be a conjugate formed by sulfotransferases or UDP-glucuronosyl transferase (sample not treated with sulfatase or  $\beta$ -glucuronidase prior to analysis). The plasma sample from volunteer 5 (lower panel) shows a detectable peak at 13.5 min, which is the retention time (top panel) of DBC-( $\pm$ )-diol. The major <sup>14</sup>C-containing peak in plasma at 3 h postdosing coelutes with parent DBC.

in our laboratory. A targeted total of 75 enrollees will be dosed with 5 nCi (46 ng) of [<sup>14</sup>C]-BaP. Plasma and urine levels of parent [<sup>14</sup>C]-BaP and [<sup>14</sup>C]-BaP metabolites will be assessed over a 72 h period employing UHPLC-AMS<sup>14</sup> (FDA IND #1117175; OSU IRB #5644). Preliminary results to date (Figure 3) show that the majority of the <sup>14</sup>C counts in plasma coelute with DBC with minor amounts of [<sup>14</sup>C]-DBC-11,12-dihydrodiol tentatively identified by coelution with unlabeled standard (synthesized and provided by Dr. Shantu Amin, Penn State University). The apparent peak eluting early (2–2.5 min) is unknown. It should be noted that this is the first sample run by UHPLC and is from plasma (not urine, where metabolites should predominant). Extraction at later time points (or pooling of some time points) and from higher volumes of

plasma should allow us to better quantify these putative metabolites.

We used a previously published PBPK model developed for the rat<sup>12</sup> to evaluate how well the human [<sup>14</sup>C]-DBC<sub>eq</sub> pharmacokinetic profile compared with that of other species. For this comparison (Figure 4), we scaled the initial step in the human metabolism of DBC from rate constants determined from rats. Otherwise, the human PBPK model was based upon average anatomy and physiology of a 70 kg adult male under the dosing conditions used in this study. When human metabolism was scaled from the rat, the PBPK simulation of parent DBC pharmacokinetics in plasma was remarkably close to the measured data during the first 12 h postdosing. At later time points, the model simulations of DBC kinetics began to

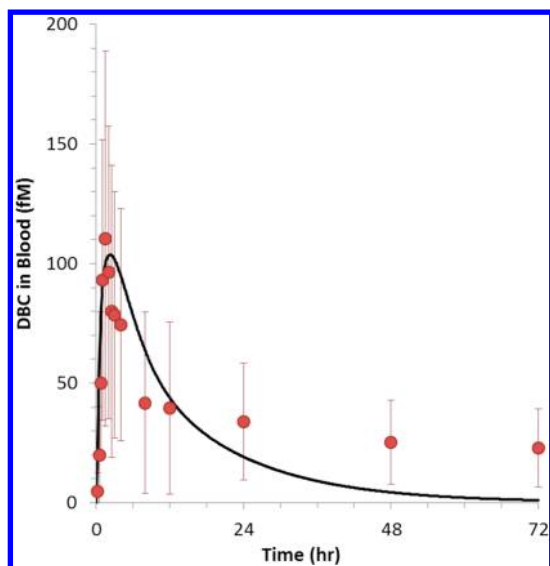


**Figure 4.** Pharmacokinetic profile of  $[^{14}\text{C}]\text{-DBC}_{\text{eq}}$  in humans: comparison to a rat PBPK model. The ● symbols are plasma levels over time of  $[^{14}\text{C}]\text{-DBC}_{\text{eq}}$  (with error bars depicting  $\pm$  SD) following microdosing of humans with 5 nCi (29 ng) of  $[^{14}\text{C}]\text{-DBC}$ . The solid curve is PBPK model prediction with metabolic rate scaled from the rat as calculated by Crowell et al.<sup>11</sup>

significantly under predict the total  $^{14}\text{C}$  data, which likely represented an increasing proportion of DBC metabolites. As described above, studies are ongoing to quantitate DBC and its major metabolites in plasma and urine samples from this study to more directly compare with PBPK predictions. These data, along with recently published data on species differences in metabolic rate constants associated with DBC metabolism,<sup>13</sup> will be incorporated into the next generation PBPK model to improve cross-species comparisons. Nevertheless, these initial comparisons based upon simple metabolic scaling assumptions are encouraging.

The pharmacokinetics of phenanthrene (a 3-ring PAH) and its diol and tetraol metabolites have been conducted in humans following oral or inhalation exposure to 10  $\mu\text{g}$  of  $[\text{D}_{10}]$ -phenanthrene and analysis of plasma and urine over time by GC-electron impact-MS/MS.<sup>49–51</sup> Phenanthrene can act as a surrogate for larger molecular weight carcinogenic PAHs<sup>52</sup> as it has a bay region and is metabolized in a manner similar to that of BaP but is designated a class C PAH by IARC<sup>1</sup> and has been given an RPF of 0 by EPA.<sup>53</sup> In our subsequent studies characterizing the pharmacokinetics of BaP and its metabolites by UHPLC-AMS following microdosing with 46 ng, we hope to examine the impact of genetic polymorphisms in BaP-metabolizing enzymes as was done by Wang et al.<sup>50</sup> Likewise, we plan to examine  $[^{14}\text{C}]\text{-PAH}$ -derived DNA and protein adducts from peripheral blood mononuclear cells (PBMCs) as potential biomarkers of exposure and perhaps risk following microdosing. The use of moving wire technology may provide the opportunity to identify macromolecular adduct profiles.

The ability to determine the pharmacokinetic parameters, safely in humans, of carcinogenic chemicals found in the environment and their metabolites is an advancement in risk assessment. Further development and application of this technology could have a major impact in the arena of human environmental health.

## AUTHOR INFORMATION

### Corresponding Author

\*Phone: 541-737-3277. E-mail: david.williams@oregonstate.edu.

### Funding

This study was funded by PHS grants P42ES016465, K.C. Donnelly Supplement P42ES016465, P41GM103483, and T32ES07060. AMS was performed at the Research Resource for Biomedical AMS, which is operated at LLNL under the auspices of the U.S. Department of Energy under contract DE-AC52-07NA27344 and National Institute of General Medical Sciences 8P41 GM103483-14.

### Notes

The authors declare no competing financial interest.

## ACKNOWLEDGMENTS

We acknowledge the pharmaceutical expertise and contribution of materials provided by Dr. Mark Christensen (College of Pharmacy, Oregon State University).

## ABBREVIATIONS

ACN, acetonitrile; AMS, accelerator mass spectrometry; ATSDR, Agency for Toxic Substances and Disease Registry; BaP, benzo[*a*]pyrene; BMI, body mass index; DBC, dibenzo[*def,p*]chrysene; DBCDE, dibenzo[*def,p*]chrysene-11,12-dihydrodiol-13,14-epoxide;  $\text{DBC}_{\text{eq}}$ , dibenzo[*def,p*]chrysene equivalents (DBC plus metabolites); DDT, 1,1,1-trichloro-2,2-di(4-chlorophenyl)ethane; GSTs, glutathione-S-transferases; HPLC, high pressure liquid chromatography; IARC, International Agency for Research on Cancer; JECFA, Joint FAO/WHO Expert Committee on Food Additives; LLNL, Lawrence Livermore National Laboratory; MeIQ, 2-amino-3,4-dimethylimidazo[4,5-*f*]quinoline; MeIQx, 2-amino-3,8-dimethylimidazo[4,5-*f*]quinoxaline; OSU, Oregon State University; PAH, polycyclic aromatic hydrocarbon; PBPK, physiologically based pharmacokinetic model; PhIP, 2-amino-1-methyl-6-phenylimidazo[4,5-*b*]pyridine; PCBs, polychlorinated biphenyls; SD, standard deviation; SULTs, sulfotransferases; TCDD, 2,3,7,8-tetrachlorodibenzo-*p*-dioxin; UGTs, UDP-glucuronosyltransferases

## REFERENCES

- (1) IARC (2010) *Monographs on the Evaluation of Carcinogenic Risks to Humans, Some Non-Heterocyclic Polycyclic Aromatic Hydrocarbons and Some Exposures*, World Health Organization International Agency for Research on Cancer, Lyon, France.
- (2) ATSDR (2013) *Priority List of Hazardous Substances*, Agency for Toxic Substances and Disease Registry, Center for Disease Control, [http://www.atsdr.cdc.gov/spl/resources/ATSDR\\_2013\\_SPL\\_Detailed\\_Data\\_Table.pdf](http://www.atsdr.cdc.gov/spl/resources/ATSDR_2013_SPL_Detailed_Data_Table.pdf).
- (3) IARC (1983) *Monographs on the Evaluation of Carcinogenic Risks to Humans, Polynuclear Aromatic Compounds, Part 1: Chemical, Environmental, and Experimental Data*, World Health Organization International Agency for Research on Cancer, Lyon, France.
- (4) Dennis, M. J., Massey, R. C., Cripps, G., Venn, I., Howarth, N., and Lee, G. (1991) Factors affecting the polycyclic aromatic hydrocarbon content of cereals, fats and other food-products. *Food Addit. Contam.* 8, 517–530.
- (5) Jakszyn, P., Agudo, A., Ibanez, R., Garcia-Closas, R., Pera, G., Amiano, P., and Gonzalez, C. A. (2004) Development of a food database of nitrosamines, heterocyclic amines, and polycyclic aromatic hydrocarbons. *J. Nutr.* 134, 2011–2014.

- (6) Santodonato, J., Howard, P., and Basu, D. (1981) Health and ecological assessment of polynuclear aromatic hydrocarbons. *J. Environ. Pathol. Toxicol.* 5, 1–364.
- (7) Hattemerfrey, H. A., and Travis, C. C. (1991) Benzo(a)pyrene environmental partitioning and human exposure. *Toxicol. Indust. Health* 7, 141–157.
- (8) Kazerouni, N., Sinha, R., Hsu, C. H., Greenberg, A., and Rothman, N. (2001) Analysis of 200 food items for benzo[a]pyrene and estimation of its intake in an epidemiologic study. *Food Chem. Toxicol.* 39, 423–436.
- (9) JECFA (2005) *Sixty-fourth International Meeting Abstracts*, Joint Food and Agriculture Organization/World Health Organization Expert Committee on Food Additives, Rome, Italy.
- (10) Menzie, C. A., Potocki, B. B., and Santodonato, J. (1992) Exposure to carcinogenic PAHs in the environment. *Environ. Sci. Technol.* 26, 1278–1284.
- (11) Veyrand, B., Sirot, V., Durand, S., Pollono, C., Matchand, P., Dervilly-Pinel, G., Tard, A., Leblanc, J. C., and Le Bizec, B. (2013) Human dietary exposure to polycyclic aromatic hydrocarbons: Results of the second French total diet study. *Environ. Int.* 54, 11–17.
- (12) Crowell, S. R., Amin, S. G., Anderson, K. A., Krishnegowda, G., Sharma, A. K., Soelberg, J. J., Williams, D. E., and Corley, R. A. (2011) Preliminary physiologically based pharmacokinetic models for benzo[a]pyrene and dibenzo[def,p]chrysene in rodents. *Toxicol. Appl. Pharmacol.* 257, 365–376.
- (13) Crowell, S. R., Sharma, A. K., Amin, S., Soelberg, J. J., Sadler, N. C., Wright, A. T., Baird, W. M., Williams, D. E., and Corley, R. A. (2013) Impact of pregnancy on the pharmacokinetics of dibenzo[def,p]chrysene in mice. *Toxicol. Sci.* 135, 48–62.
- (14) Brown, K., Tompkins, E. M., and White, I. N. H. (2006) Applications of accelerator mass spectrometry for pharmacological and toxicological research. *Mass Spectrom. Rev.* 25, 127–145.
- (15) Forsgard, N., Salehpour, M., and Possnert, G. (2010) Accelerator mass spectrometry in the attomolar concentration range for <sup>14</sup>C-labeled biologically active compounds in complex matrices. *J. Anal. At. Spectrom.* 25, 74–78.
- (16) Dueker, S. R., Lohstroh, P. N., Giacomo, J. A., Le, T. V., Keck, B. D., and Vogel, J. S. (2010) Early human ADME using microdoses and microtracers: bioanalytical considerations. *Bioanalyt.* 2, 441–454.
- (17) Dueker, S. R., Vuong, L. T., Lohstroh, P. N., Giacomo, J. A., and Voegel, J. S. (2011) Quantifying exploratory low dose compounds in humans with AMS. *Adv. Drug Delivery Rev.* 63, 518–531.
- (18) Penner, N., Xu, L., and Prakash, C. (2012) Radiolabeled absorption, distribution, metabolism, and excretion studies in drug development: why, when, and how? *Chem. Res. Toxicol.* 25, 513–531.
- (19) Dingley, K. H., Curtis, K. D., Nowell, S., Felton, J. S., Lang, N. P., and Turteltaub, K. W. (1999) DNA and protein adduct formation in the colon and blood of humans after exposure to a dietary-relevant dose of 2-amino-1-methyl-6-phenylimidazo [4,5-b] pyridine. *Cancer Epidemiol. Biomarkers Prev.* 8, 507–512.
- (20) Dingley, K. H., Freeman, S., Nelson, D. O., Garner, R. C., and Turteltaub, K. W. (1998) Covalent binding of 2-amino-3,8-dimethylimidazo [4,5-f] quinoxaline to albumin and hemoglobin at environmentally relevant doses - Comparison of human subjects and F344 rats. *Drug Metab. Dispos.* 26, 825–828.
- (21) Garner, R. C., Lightfoot, T. J., Cupid, B. C., Russell, D., Coxhead, J. M., Kutschera, W., Priller, A., Rom, W., Steier, P., Alexander, D. J., Leveson, S. H., Dingley, K. H., Mauthe, R. J., and Turteltaub, K. W. (1999) Comparative biotransformation studies of MeIQx and PhIP in animal models and humans. *Cancer Lett.* 143, 161–165.
- (22) Lang, N. P., Nowell, S., Malfatti, M. A., Kulp, K. S., Knize, M. G., Davis, C., Massengill, J., Williams, S., MacLeod, S., Dingley, K. H., Felton, J. S., and Turteltaub, K. W. (1999) *In vivo* human metabolism of [2-<sup>14</sup>C]2-amino-1-methyl-6-phenylimidazo-[4,5-b] pyridine (PhIP). *Cancer Lett.* 143, 135–138.
- (23) Lightfoot, T. J., Coxhead, J. M., Cupid, B. C., Nicholson, S., and Garner, R. C. (2000) Analysis of DNA adducts by accelerator mass spectrometry in human breast tissue after administration of 2-amino-1-methyl-6-phenylimidazo [4,5-b] pyridine and benzo[a]pyrene. *Mutat. Res., Genet. Toxicol. Environ. Mutagen.* 472, 119–127.
- (24) Jubert, C., Mata, J., Bench, G., Dashwood, R., Pereira, C., Tracewell, W., Turteltaub, K., Williams, D., and Bailey, G. (2009) Effects of chlorophyll and chlorophyllin on low-dose aflatoxin B<sub>1</sub> pharmacokinetics in human volunteers. *Cancer Prev. Res.* 2, 1015–1022.
- (25) Castro, D. J., Baird, W. M., Pereira, C. B., Giovanini, J., Löhr, C. V., Fischer, K. A., Yu, Z., Gonzalez, F. J., Krueger, S. K., and Williams, D. E. (2008) Fetal mouse Cyp1b1 and transplacental carcinogenesis from maternal exposure to dibenzo(a,l)pyrene. *Cancer Prev. Res.* 1, 128–134.
- (26) Castro, D. J., Löhr, C. V., Fischer, K. A., Pereira, C. B., and Williams, D. E. (2008) Lymphoma and lung cancer in offspring born to pregnant mice dosed with dibenzo[a,l]pyrene: The importance of *in utero* vs. lactational exposure. *Toxicol. Appl. Pharmacol.* 233, 454–458.
- (27) Castro, D. J., Yu, Z., Löhr, C. V., Pereira, C. B., Giovanini, J. N., Fischer, K. A., Orner, G. A., Dashwood, R. H., and Williams, D. E. (2008) Chemoprevention of dibenzo[a,l]pyrene transplacental carcinogenesis in mice born to mothers administered green tea: primary role of caffeine. *Carcinogenesis* 29, 1581–1586.
- (28) Castro, D. J., Löhr, C. V., Fischer, K. A., Waters, K. M., Webb-Robertson, B. J., Dashwood, R. H., Bailey, G. S., and Williams, D. E. (2009) Identifying efficacious approaches to chemoprevention with chlorophyllin, purified chlorophylls and freeze-dried spinach in a mouse model of transplacental carcinogenesis. *Carcinogenesis* 30, 315–320.
- (29) Shorey, L. E., Castro, D. J., Baird, W. M., Siddens, L. K., Löhr, C. V., Matzke, M. M., Waters, K. M., Corley, R. A., and Williams, D. E. (2012) Transplacental carcinogenesis with dibenzo[def,p]chrysene (DBC): Timing of maternal exposures determines target tissue response in offspring. *Cancer Lett.* 317, 49–55.
- (30) Yu, Z., Loehr, C., Fischer, K. A., Louderback, M., Krueger, S. K., Dashwood, R. H., Kerkvliet, N. I., Pereira, C. B., Jennings-Gee, J., Dance, S. T., Miller, M. S., Bailey, G. S., and Williams, D. E. (2006) *In utero* exposure of mice to dibenzo[a,l]pyrene produces lymphoma in the offspring: role of the aryl hydrocarbon receptor. *Cancer Res.* 66, 755–762.
- (31) Yu, Z., Mahadevan, B., Löhr, C. V., Fischer, K. A., Louderback, M. A., Krueger, S. K., Pereira, C. B., Albershardt, D. J., Baird, W. M., Bailey, G. S., and Williams, D. E. (2006) Indole-3-carbinol in the maternal diet provides chemoprotection for the fetus against transplacental carcinogenesis by the polycyclic aromatic hydrocarbon, dibenzo[a,l]pyrene. *Carcinogenesis* 27, 2116–2123.
- (32) BinSamat, S., Green, S., and Beddoe, A. H. (1997) The K-40 activity of one gram of potassium. *Phys. Med. Biol.* 42, 407–413.
- (33) Savarino, V., Vigneri, S., and Celle, G. (1999) The <sup>14</sup>C urea breath test in the diagnosis of *Helicobacter pylori* infection. *Gut* 45, 118–122.
- (34) (1997) Council Directive 97/43/Euratom on Health Protection of Individuals against the Dangers of Ionizing Radiation InRelation ToMedical Exposure, and Repealing Directive 84/466/Euratom, Council of Federal Regulations 10 part 20.10003.
- (35) Crowell, S. R., Hanson-Drury, S., Williams, D. E., and Corley, R. A. (2014) *In vitro* metabolism of benzo[a]pyrene and dibenzo[def,p]chrysene in rodent and human hepatic microsomes. *Toxicol. Lett.* 228, 48–55.
- (36) Ognibene, T. J., Bench, G., Vogel, J. S., Peaslee, G. F., and Murov, S. (2003) A high-throughput method for the conversion of CO<sub>2</sub> obtained from biochemical samples to graphite in septa-sealed vials for quantification of C-14 via accelerator mass spectrometry. *Anal. Chem.* 75, 2192–2196.
- (37) Ognibene, T. J., Bench, G., Brown, T. A., and Vogel, J. S. (2004) The LLNL accelerator mass spectrometry system for biochemical <sup>14</sup>C-measurements. *Nucl. Instrum. Methods Phys. Res.* 23, 12–15.
- (38) Ognibene, T. J., and Salazar, G. A. (2013) Installation of hybrid ion source on the 1-MV LLNL BioAMS spectrometer. *Nucl. Instrum. Methods Phys. Res., Sect. B* 294, 311–314.

(39) Usansky, J., Desai, A., and Tang-Liu, D. (2005) *PK Functions for Microsoft Excel*, Department of Pharmacokinetics and Drug Metabolism, Allergan, Irvine, CA.

(40) Gibaldi, M., and Perrier, D. (1982) Noncompartmental analysis based on statistical moment theory. *Pharmacokin* 2, 409–417.

(41) Rahman, A., Barrowman, J. A., and Rahimtula, A. (1986) The influence of bile on the availability of polynuclear aromatic hydrocarbons from the rat intestine. *Can. J. Physiol. Pharmacol.* 64, 1214–1218.

(42) Harris, D. L., Hood, D. B., and Ramesh, A. (2008) Vehicle-dependent disposition kinetics of fluoranthene in Fisher-344 rats. *Int. J. Environm. Res. Public Health* 5, 41–48.

(43) Jongeneelen, F. J., Leijdekkers, C. M., and Henderson, P. T. (1984) Urinary-excretion of 3-hydroxy-benzo[*a*]pyrene after percutaneous penetration and oral absorption of benzo[*a*]pyrene in rats. *Cancer Lett.* 25, 195–201.

(44) Bouchard, M., and Viau, C. (1997) Urinary excretion of benzo[*a*] pyrene metabolites following intravenous, oral, and cutaneous benzo[*a*]pyrene administration. *Can. J. Physiol. Pharmacol.* 75, 185–192.

(45) Baird, W. M., Hooven, L. A., and Mahadevan, B. (2005) Carcinogenic polycyclic aromatic hydrocarbon-DNA adducts and mechanism of action. *Environm. Mol. Mutagen.* 45, 106–114.

(46) Shimada, T. (2006) Xenobiotic-metabolizing enzymes involved in activation and detoxication of carcinogenic polycyclic aromatic hydrocarbons. *Drug Metabol. Pharmacokin.* 21, 257–276.

(47) Mahadevan, B., Dashwood, W.-M., Luch, A., Pecaj, A., Doehmer, J., Seidel, A., Pereira, C., and Baird, W. M. (2003) Mutations induced by (–)-*anti*-11*R*,12*S*-dihydrodiol-13*S*,14*R*-epoxide of dibenzo[*a,l*]pyrene in the coding region of the hypoxanthine phosphoribosyltransferase (Hprt) gene in Chinese hamster V79 cells. *Environ. Mol. Mutagen.* 41, 131–139.

(48) Thomas, A. T., Stewart, B. J., Ognibene, T. J., Turteltaub, K. W., and Bench, G. (2013) Directly coupled high-performance liquid chromatography-accelerator mass spectrometry measurement of chemically modified protein and peptides. *Anal. Chem.* 85, 3644–3650.

(49) Zhong, Y., Wang, J., Carmella, S. G., Hochalter, J. B., Rauch, D., Oliver, A., Jensen, J., Hatsukami, D. K., Upadhyaya, P., Zimmerman, C., and Hecht, S. S. (2011) Metabolism of [D<sub>10</sub>]phenanthrene to tetraols in smokers for potential lung cancer susceptibility assessment: comparison of oral and inhalation routes of administration. *J. Pharmacol. Exp. Ther.* 338, 353–361.

(50) Wang, J., Zhong, Y., Carmella, S. G., Hochalter, J. B., Rauch, D., Oliver, A., Jensen, J., Hatsukami, D. K., Upadhyaya, P., Hecht, S. S., and Zimmerman, C. L. (2012) Phenanthrene metabolism in smokers: use of a two-step diagnostic plot approach to identify subjects with extensive metabolic activation. *J. Pharmacol. Exp. Ther.* 342, 750–760.

(51) Hecht, S. S., Hochalter, J. B., Carmella, S. G., Zhang, Y., Rauch, D. M., Fujioka, N., Nensen, J., and Hatsukami, D. K. (2013) Longitudinal study of [D<sub>10</sub>]phenanthrene metabolism by the diol epoxide pathway in smokers. *Biomarkers* 18, 144–150.

(52) Hecht, S. S., Carmella, S. G., Villalta, P. W., and Hochalter, J. B. (2010) Analysis of phenanthrene and benzo[*a*]pyrene tetraol enantiomers in human urine: relevance to the bay region diol epoxide hypothesis of benzo[*a*]pyrene carcinogenesis and to biomarker studies. *Chem. Res. Toxicol.* 23, 900–908.

(53) U.S. EPA (2010) Development of a Relative Potency Factor (RPF) Approach for Polycyclic Aromatic Hydrocarbon (PAH) Mixtures (External Review Draft), EPA/635/R-08/012A, U.S. EPA, Washington, D.C.